Title
FELIX ACCEPTANCE STUDIES

Authors
Garren, Alper A.
Hiskes, John R.
Northrop, Ted G.
et al.

Publication Date
1958-01-22

UCRL 8140

DECLASSIFIED

UNIVERSITY OF CALIFORNIA

Radiation Laboratory

BERKELEY, CALIFORNIA

DISCLAIMER

UNIVERSITY OF CALIFORNIA
Radiation Laboratory

Cover Sheet
Do not remove

INDEX NO. UCRL-8140
This document contains 21 pages
This is copy 7 of 7 series A
Date 1-22-58

DECLASSIFIED

Issued to Info. Div., Berkeley

[redacted]
Classification

Each person who receives this document must sign the cover sheet in the space below.

Route to	Noted by	Date	Route to	Noted by	Date
	R.C. McRae	3-11-58			
	Morris	3-17-58			
	Reed Maynard	3/18/58			
UCRL LIVERMORE		✓			
UCRL LIVERMORE		✓			

RL-220

DECLASSIFIED

~~SECRET~~

UCRL-8140

UNIVERSITY OF CALIFORNIA

Radiation Laboratory
Berkeley, California

Contract No. W-7405-eng-48

CLASSIFICATION CANCELLED
BY AUTHORITY OF THE DECLASSIFICATION BRANCH USAEC ON 8-21-58
DATE
By B Foskett
SIGNATURE OF THE PERSON MAKING THE CHANGE

FELIX ACCEPTANCE STUDIES

Alper A. Garren, John R. Hiskes, Ted G. Northrop, and Lloyd Smith

January 22, 1958

~~RESTRICTED DATA~~

~~This document contains restricted data as defined in the~~ Atomic Energy Act of 1954. ~~Its transmittal~~ or the disclosure of its con~~tents in any~~ manner to an unauthorized person is prohibited.

49655

Printed for the U.S. Atomic Energy Commission

~~SECRET~~

DECLASSIFIED

DECLASSIFIED

UCRL-8140

[redacted]

FELIX ACCEPTANCE STUDIES

by

Alper A. Garren, John R. Hiskes, Ted G. Northrop, and Lloyd Smith

Radiation Laboratory
University of California
Berkeley and Livermore California

This report presents a theoretical estimate of the acceptance time in Felix, taking into account the non-adiabatic and precessional effects indicated by orbit computations. Our knowledge of these effects is by no means complete; for example, it will be seen that our results depend on the assumption that the magnetic moment is constant with respect to time variation in the magnetic field. The predictions of this report have been subjected to spot checks consisting of computations of specific orbits in the time-varying Felix field. These checks lead us to believe that our development should provide an adequate picture of the factors influencing end injection in a mirror machine.

INTRODUCTION

At the Berkeley Sherwood meeting a report was given describing certain machine calculations of orbits in a mirror field similar to that of Felix.[1] The important results were that the magnetic moment is by no means a constant, that its departure from constancy is a sharply increasing function of the radius of curvature; but that for any particle velocity an effective loss cone exists and is defined by a minimum-pitch angle (which is an increasing function of particle energy) such that when the pitch angle is less than this minimum the variations in the magnetic moment are more or less random, leading to loss through the ends, whereas when the pitch angle is larger than the minimum the variations in the magnetic moment are oscillatory, leading apparently to stable motion inside the mirrors. Because experiments on end injection in Felix have now begun, and because the earlier analyses by Post[2, 3] of end injection were made before these properties of the orbits were known, we thought it desirable to make a new study of end injections

DECLASSIFIED

[redacted]

incorporating the new data about orbits in order to help determine optimal injection conditions, to help interpret experimental observations, and to give some rough estimates of what might, under certain assumed conditions be observed experimentally.

LOSS CONE AND CLEARANCE ON FIRST TURN

An absolute upper limit to the acceptance time for constant injection energy and with a given source position may be obtained by determining the maximum radius of curvature leading to orbits outside the true (nonadiabatic) loss cone, and the minimum radius of curvature required to miss the source on the first turn. Figure 1 shows how these quantities depend on source position z_s for injection normal to a field with axial component of the form

$$H_z = H_0 \left[1 - \alpha I_0 \left(\frac{2\pi r}{L}\right) \cos \left(\frac{2\pi z}{L}\right)\right] . \tag{1}$$

Here L is the distance between mirrors, and the on-axis mirror ratio is given by $(1 + \alpha)/(1 - \alpha)$. For the Felix mirror ratio of 1.5 one has $\alpha = 0.20$. The ordinate V is a dimensionless parameter, $(2\pi/L)(Mcv/eH_0)$, representing particle speed and expressing approximately the radius of curvature, ρ, of the orbit, compared with machine dimensions:[a]

$$V \sim 2\pi \frac{\rho}{L} .$$

The line marked "stable-unstable" marks the loss cone, and is derived from the machine computations at $V = 0.6$, 0.4, and 0.2. The lower curves marked with various values of Δz are obtained from the adiabatic expression for displacement parallel to the field in one turn, for injection perpendicular to the field lines:[4]

$$\Delta z = - \pi^2 \rho^2 \frac{1}{H} \frac{dH}{dz} \sim -\left(\frac{LV}{2}\right)^2 \frac{1}{H} \frac{dH}{dz} , \tag{2}$$

where ρ is the radius of curvature at the source and the derivative is with respect to the field direction at the source. All these curves really depend also on the radial position of the source and angle of injection in the plane transverse to the field line through the source, but our impression is that the variation is not large.

The parameter V is uniquely related to the time at which the particle is injected by the formula

$$V = \frac{2\pi}{L} v \frac{Mc}{eH_0(t)} \sim \frac{2\pi}{L} v \frac{Mc}{e\dot{H}_0(0) t} \sim \frac{160 \times 10^{-6}}{t} . \tag{3}$$

[a] V is exactly $2\pi\rho/L$ for a particle being reflected on axis at $z = L/4$.

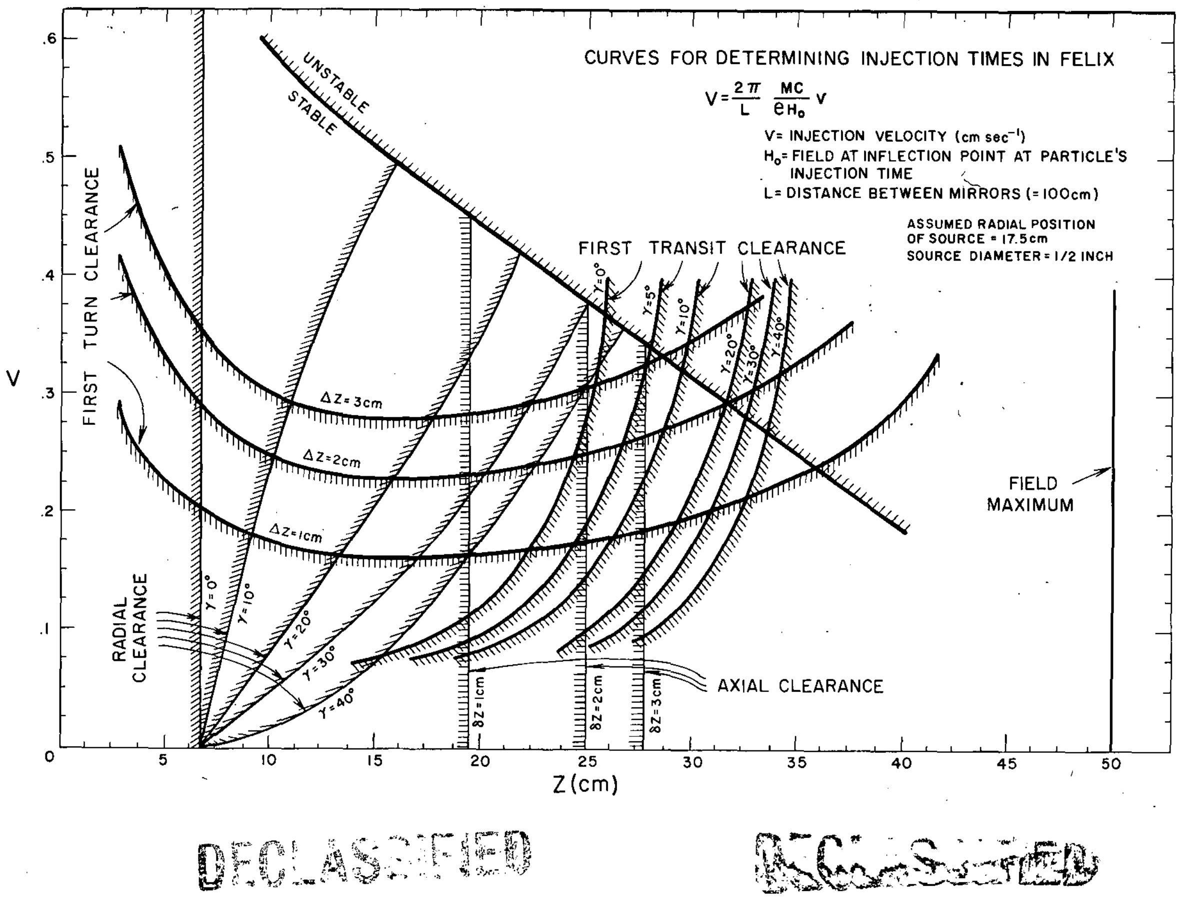
CURVES FOR DETERMINING INJECTION TIMES IN FELIX
V = 2π/L MC/eH₀ v
V = INJECTION VELOCITY (cm sec⁻¹)
H₀ = FIELD AT INFLECTION POINT AT PARTICLE'S INJECTION TIME
L = DISTANCE BETWEEN MIRRORS (= 100cm)
ASSUMED RADIAL POSITION OF SOURCE = 17.5cm
SOURCE DIAMETER = 1/2 INCH
UNSTABLE
STABLE
FIRST TURN CLEARANCE
FIRST TRANSIT CLEARANCE
RADIAL CLEARANCE
AXIAL CLEARANCE
FIELD MAXIMUM
ΔZ = 3cm
ΔZ = 2cm
ΔZ = 1cm
δZ = 1cm
δZ = 2cm
δZ = 3cm
γ = 0°
γ = 5°
γ = 10°
γ = 20°
γ = 30°
γ = 40°
V
Z (cm)
0
.1
.2
.3
.4
.5
.6
5
10
15
20
25
30
35
40
45
50
DECLASSIFIED

Fig. 1.

The numerical value is based on 10-kev deuterons, a sinusoidal rise of field at the center of 20,000 gauss in 4.8 msec, and a length of 100 cm. Thus the earliest and latest injection times for given source position and extent of source structure to be cleared can be computed from the appropriate V_{max} and V_{min}. Table I gives these times for various source positions. It can be seen that the average effective time decreases gradually with increasing distance from the center plane.

PRECESSIONAL EFFECTS AND ADIABATIC TRAPPING

It should be realized that these phenomena cannot be used to extend the times given in Table I, but rather serve to insure usefulness of a sizeable fraction of those times. There are three major points to consider here; clearing the source on the first transit, and clearing in z or r after a complete precession cycle. In order to discuss them, one needs a quantitative measure of precession. The solid curve of Fig. 2 is the adiabatic result; i.e., the integral of the lateral drift velocity[5] for one round-trip transit in the Felix field. The relevant formula is

$$\Delta\theta = \frac{2Mcv}{e} \int_0^{z_s} \frac{\frac{1}{rH}\frac{dH}{dr}}{\sqrt{H_s(H_s - H)}}\, dz \approx \sqrt{2a}\,V \frac{2E(\sin\frac{\pi z_s}{L}) - K(\sin\frac{\pi z_s}{L})}{\left(1 - a\cos\frac{2\pi z_s}{L}\right)^{3/2}}, \qquad (4)$$

where E(k) and K(k) are complete elliptic integrals.

The lettered points represent the corresponding numbers available from the exact orbit computations. It can be seen that the adiabatic approximation represents the truth moderately well, and accordingly we have chosen to represent the precession per transit by a straight-line approximation,

$$\Delta\theta = V\left[1.66 - 0.044z\right], \qquad (5)$$

where $\Delta\theta$ is in radians and z in centimeters.
The precession undoubtedly depends also on the radial position of the guiding center, but the one exact orbit we have following a different flux tube shows a precession falling within the scatter of the other points in Fig. 2. Since the adiabatic calculation also indicates only a weak dependence, we shall adopt Eq. (5) as an adequate representation for present purposes.

Regarding the problems of missing the source on the first transit (see Fig. 3 for geometrical arrangement), we neglect the effect of the time-varying field and rely on precession only. Since the axial distance covered by an ion during the last half turn at reflection is generally small, we assume that the ion will hit the source if the projected circle

Table I

Maximum injection times (μsec) limited only by stability and first-turn clearance						
Δz (cm)	V_f	V_i	t_f	t_i	Δt (μsec)	$(\Delta t)_{Av}$ (μsec)
			z = 10 cm			
1	0.170	0.570	940	280	660	
2	0.237	0.555	680	290	390	440
3	0.285	0.537	560	300	260	
			z = 15 cm			
1	0.1625	0.495	980	320	660	
2	0.230	0.482	700	330	370	420
3	0.282	0.470	570	340	230	
			z = 20 cm			
1	0.1675	0.432	960	370	590	
2	0.238	0.420	670	380	290	340
3	0.297	0.407	540	390	150	
			z = 25 cm			
1	0.180	0.365	890	440	450	
2	0.260	0.355	620	450	170	210
3	0.327	0.342	490	470	20	
			z = 30 cm			
1	0.205	0.302	780	530	250	80
2	-	-	-	-	-	
3	-	-	-	-	-	

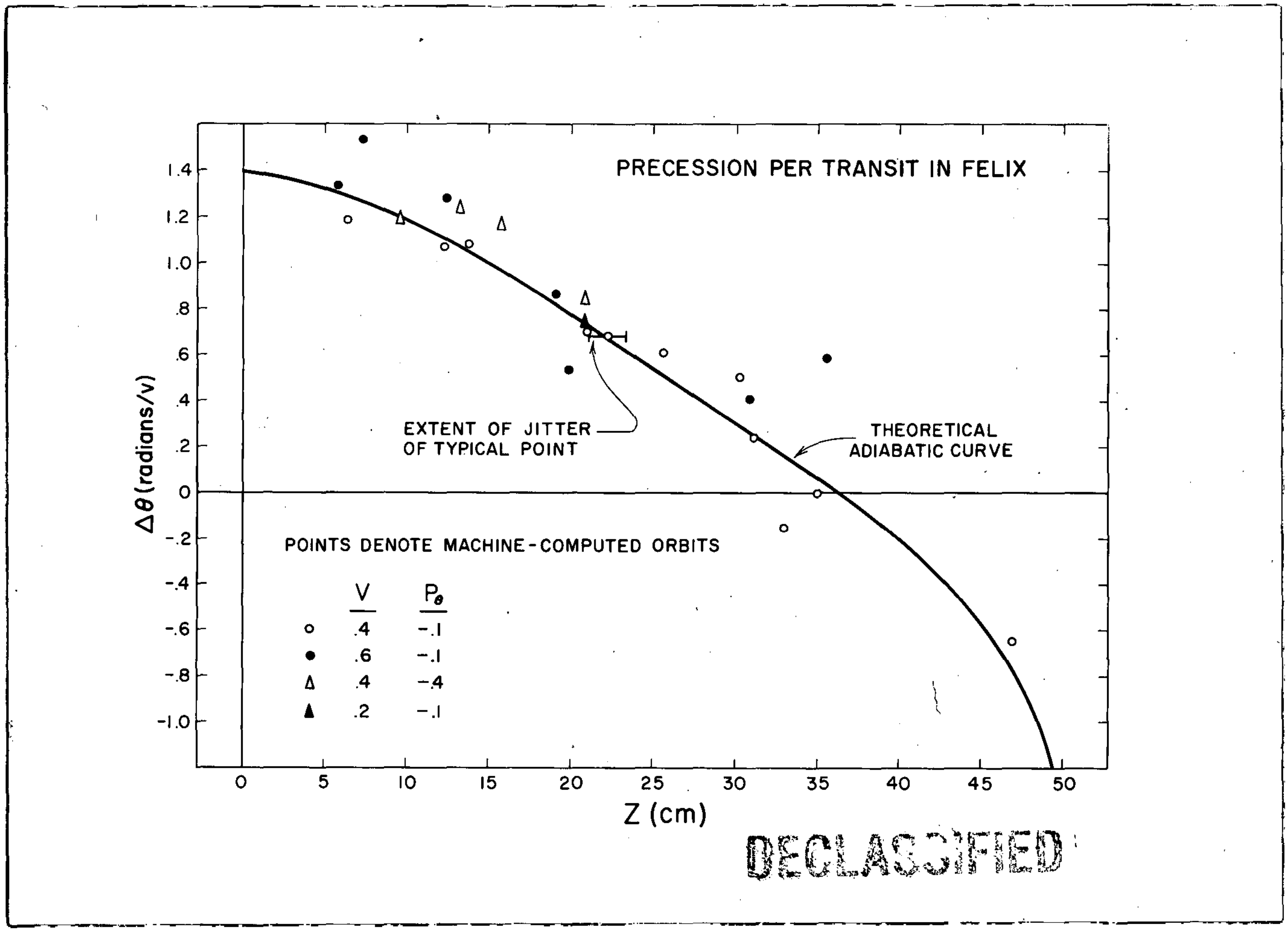

PRECESSION PER TRANSIT IN FELIX
Δθ (radians/v)
1.4
1.2
1.0
.8
.6
.4
.2
0
-.2
-.4
-.6
-.8
-1.0
EXTENT OF JITTER OF TYPICAL POINT
THEORETICAL ADIABATIC CURVE
POINTS DENOTE MACHINE-COMPUTED ORBITS
V
Pθ
.4 -.1
.6 -.1
.4 -.4
.2 -.1
0
5
10
15
20
25
30
35
40
45
50
Z (cm)
DECLASSIFIED

Fig. 2.

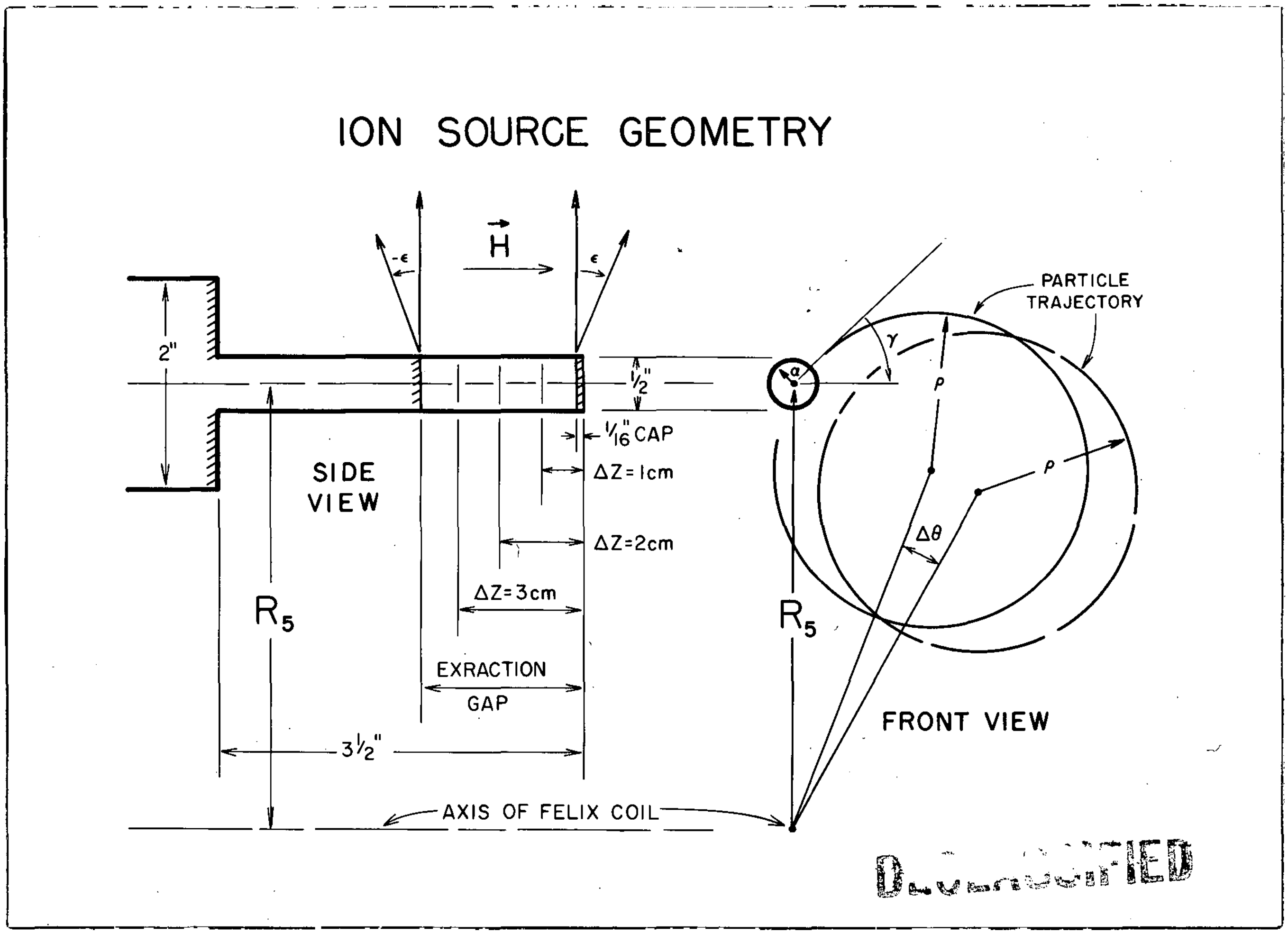
ION SOURCE GEOMETRY
H
-ε
ε
2"
½"
1/16" CAP
ΔZ=1cm
ΔZ=2cm
ΔZ=3cm
SIDE VIEW
R5
EXRACTION GAP
3½"
AXIS OF FELIX COIL
PARTICLE TRAJECTORY
α
γ
ρ
ρ
Δθ
R5
FRONT VIEW

Fig. 3.

in the transverse plane, after one transit, intersects the small circle representing the source. Analyzing the geometry of the two circles, one arrives at the following requirement for the precession angle:

$$\Delta\theta > \frac{\rho \sin\gamma}{R_s - \rho\cos\gamma}\left\{\left[1 + \frac{2a}{R_s\rho}\;\frac{R_s - \rho\cos\gamma}{\sin^2\gamma}\right]^{1/2} - 1\right\}, \qquad (6)$$

where

ρ = radius of projected circle at the source,

R_s = radial position of the source,

a = radius of the source,

γ = angle of injection in the plane normal to the field measured outward from the azimuthal direction.

Since we have $\rho \sim (L/2\pi)V$, Eqs. (5) and (6) determine a maximum permissible z for the source[b] as a function of V and the angle γ such that the precession be sufficient to insure missing on the first transit. The right-hand set of curves in Fig. 1, marked with the values of γ, gives this upper bound for $a = 1/4$ inch, $R_s = 17.5$ cm. That the limiting z increases with γ results from the fact that the source is easier to miss if the ions are projected outward.

Before discussing the significance of these limiting curves, we proceed to the adiabatic decrease in z and r after precession through an angle $2\pi/N$, N indicating either the number of sources at the same r and z, or the reciprocal of the number of 360° precessions if more than one is allowed. Under the assumption of adiabaticity, the two expressions are

$$\delta z = \frac{2\pi}{N\Delta\theta}\;\frac{4}{vt}\;\frac{1}{\left(\frac{1}{H}\frac{dH}{dz}\right)_s}\int_0^{z_s} dz\sqrt{1 - \frac{H(z,r)}{H(z_s,r_s)}} \qquad (7)$$

and

$$\frac{\delta r}{r} = \frac{2\pi}{N\Delta\theta}\;\frac{2}{vt}\int_0^{z_s}\frac{dz}{\sqrt{1 - \frac{H(z,r)}{H(z_s,r_s)}}}, \qquad (8)$$

where the subscript s refers to source position.

For H varying as $\left[1 - \alpha I_0(2\pi r/L)\cos(2\pi z/L)\right]$, Eqs. (7) and (8) are expressible in terms of elliptic integrals if the variation in radius of the position of the guiding center is ignored. It may, incidentally, be

[b]Beyond $z = 1.66/0.044 = 38$ cm, the precession reverses and the consequences are different, but the interesting region for injection seems to be well within this point.

verified that Eq. (7) agrees with the expression given by Post[2] for a uniform field terminated by short mirrors. With the addition of the precession factor, the expressions take on a new meaning, however. The shrinkage per transit depends on the fractional change in H per transit and is thus inversely proportional to the field magnitude at injection and thus ultimately to the time at injection, t. On the other hand, the precession per transit by Eqs. (3) and (5) decreases inversely as the injection time t for constant injection energy. As a result, by the time the orbit has precessed through a large angle, $2\pi/N$, the total shrinkage is independent of injection time, but only depends on the axial position of the injector, which appears explicitly in Eqs. (5), (7), and (8). One then concludes that the adiabatic shrinkage, which was previously considered as determining an injection time, determines rather a minimum z for the source depending only on the size of the source structure.

Integrating Eq. (7) and introducing (5) and (3) leads to the condition on source location to miss in z for N = 1:

$$\delta z \left[\frac{53}{z_s} - 1.40 \right] < \frac{4}{\pi} \; \frac{E(\sin x) - \cos^2 x \, K(\sin x)}{x \sin x \cos x}, \tag{9}$$

where $x = (\pi z_s/L)$, δz = length of source inward from point of injection, and K and E are the complete elliptic integrals of first and second kind. The solution of Eq. (9) is represented by vertical lines in Fig. 1.

Similarly, from Eq. (8), for N = 1, we have

$$z_s > 36 - 0.87 \, (R_s/\delta r) \, K \, (\sin x) \tag{10}$$

in order to miss in r.

Here δr is not simply the radius of the source, for if the ions are projected outward in the transverse plane, the outer edge of the circle must move in to pass under the source after precession; that is

$$\delta r = \rho \left[1 - \frac{R_s \cos \gamma - \rho}{(\rho^2 + R_s^2 - 2\rho R_s \cos \gamma)^{1/2}} \right] + a. \tag{11}$$

Combining Eqs. (10) and (11), we obtain a new family of curves of minimum allowable z as a function of V for various angles of injection, γ. These curves appear at the left side of Fig. 1. (R_s = 17.5 cm, a = 1/4 inch.)

USE OF FIGURE 1

Since Fig. 1 in its completeness consists of a somewhat confusing maze of curves to be interpreted in different ways, we shall attempt to summarize the argument up to this point before proceeding further. There are five types of curves:

(a) A single, almost straight line of negative slope marking the boundary of the nonadiabatic loss cone. Particles injected with values of V above this line will run out of the mirror or strike the source after relatively few transits.

(b) A set of curves, concave upwards, characterized by the Δz required to miss the source on the first turn. Particles injected perpendicular to the field direction at distance Δz from the leading edge of the source will strike the source on the first turn if V lies below the corresponding curve.

(c) The set of lines on the right characterized by the injection angle, γ, in the transverse plane, expressing the restriction imposed by requiring that the particles miss the source on the first transit by virtue of precession. Particles injected below and to the right of the appropriate γ curve will strike on the first transit.

(d) The set of vertical lines characterized by the required shrinkage, δz, to miss the source axially after 360° precession. Particles injected to the left of these curves will fail to clear in z after 360° precession.

(e) The set of curves to the left, characterized by γ, representing the restriction of missing the source radially after 360° precession. Particles injected with values of V and z lying to the left of these curves will fail to clear in radius after 360° precession.

Acceptance time for given $\Delta z = \delta z$, given γ, and given axial source position is obtained by reading from Fig. 1 the minimum and maximum values of V permitted by the interlacing five curves, and translating to time by the use of Expression (3). It must be remembered that only the less restrictive of Eqs. (6) and (7) need be considered, for if the ion clears axially its radial position does not matter, and vice versa. In this manner we arrive at Table II, giving the earliest and latest injection times and the differences for various source positions and values of γ and $\Delta z = \delta z$.

For a source injecting over a range of $\pm 20^\circ$ in γ it would appear that the optimum occurs at about z = 20 cm with the source oriented to

Table II

Injection times limited by first-turn clearance, stability, first-transit precessional clearance, and axial or radial adiabatic shrinkage in one precessional period.

	γ	V_f	V_i	t_f	t_i	Δt (μsec)	$(\Delta t)_{Av}$ (over γ) (μsec)
				z = 10 cm			
Δz = 1 cm	0	0.170	0.570	940	280	660	
	10	0.170	0.292	940	550	390	
	20	--	--	--	--	--	
	30	--	--	--	--	--	
	40	--	--	--	--	--	180
Δz = 2 cm	0	0.237	0.555	670	290	380	
	10	0.237	0.342	670	470	200	
	20	--	--	--	--	--	
	30	--	--	--	--	--	
	40	--	--	--	--	--	100
Δz = 3 cm	0	0.285	0.537	560	300	260	
	10	0.285	0.384	560	420	140	
	20	--	--	--	--	--	
	30	--	--	--	--	--	
	40	--	--	--	--	--	70
					Average(over Δz)		120
				z = 15 cm			
Δz = 1 cm	0	0.1625	0.495	980	320	660	
	10	0.1625	0.495	980	320	660	
	20	0.1625	0.232	980	690	290	
	30	--	--	--	--	--	
	40	--	--	--	--	--	320
Δz = 2 cm	0	0.230	0.482	700	330	370	
	10	0.230	0.482	700	330	370	
	20	0.230	0.257	700	620	80	
	30	--	--	--	--	--	
	40	--	--	--	--	--	160

Table II (cont.)

	γ	V_f	V_i	t_f	t_i	Δt (μsec)	$(\Delta t)_{Av}$ (over γ) (μsec)
				z = 15 cm (cont.)			
Δz = 3 cm	0	0.282	0.470	570	340	230	
	10	0.282	0.470	570	340	230	
	20	0.282	0.285	570	560	10	
	30	--	--	--	--	--	
	40	--	--	--	--	--	90
					Average(over Δz)		190
				z = 20 cm			
Δz = 1 cm	0	0.1675	0.432	960	370	590	
	10	0.1675	0.432	960	370	590	
	20	0.1675	0.432	960	370	590	
	30	0.1675	0.432	960	370	590	
	40	0.1675	0.432	960	370	590	590
Δz = 2 cm	0	0.238	0.420	670	380	290	
	10	0.238	0.420	670	380	290	
	20	0.238	0.420	670	380	290	
	30	0.238	0.280	670	570	100	
	40	-	-	-	-	-	210
Δz = 3 cm	0	0.297	0.407	540	390	150	
	10	0.297	0.407	540	390	150	
	20	0.297	0.407	540	390	150	
	30	0.297	0.308	540	520	20	100
	40	-	-	-	-	-	
					Average (over Δz)		300
				z = 25 cm			
Δz = 1 cm	0	-	-	-	-	-	
	10	0.180	0.365	890	440	450	
	20	0.180	0.365	890	440	450	
	30	0.180	0.365	890	440	450	
	40	0.180	0.365	890	440	450	450
Δz = 2 cm	0	-	-	-	-	-	
	10	0.260	0.355	620	450	170	
	20	0.260	0.355	620	450	170	
	30	0.260	0.355	620	450	170	
	40	0.260	0.355	620	450	170	170

Table II (cont.)

	γ	V_f	V_i	t_f	t_i	Δt (μsec)	$(\Delta t)_{Av}$(over γ) (μsec)
				z = 25 cm (cont.)			
Δz = 3 cm	0	-	-	-	-	-	
	10	0.327	0.342	490	470	20	
	20	0.327	0.342	490	470	20	
	30	0.327	0.342	490	470	20	
	40	0.327	0.342	490	470	20	20
					Average(over Δz)		210
				z = 30 cm			
Δz = 1 cm	0	-	-	-	-	-	
	10	-	-	-	-	-	
	20	0.263	0.302	610	530	80	
	30	0.210	0.302	760	530	230	
	40	0.203	0.302	790	530	260	180
Δz = 2 cm	all γ						0
Δz = 3 cm	all γ						0
					Average (over Δz)		60

give an average outward angle of about 20°. It would also appear that the rear half of the source is not very effective; if, for instance, neutral gas accompanying the ion current presents a serious problem one might just as well block off the rear half of the source. One can also extract an effective injection time from Table II--that is, a time which, when multiplied by the total source current, gives the total injected charge. At an axial source position of 20 cm this is about 300 μsec for optimum average γ, tapering off to about 200 μsec at 15 and 25 cm. The 200-μsec figure is more uncertain, for the optimum orientation appears to involve values of γ beyond the range of Fig. 1.

EFFECT OF INJECTING AT AN ANGLE TO THE NORMAL TO THE FIELD

The foregoing numerical work is based on injection normal to the field lines. Apparently not much is known about the source distribution in angle with respect to the field lines except that the ends of the beam fan out to about 15° from the normal to the field line at the source. On the suspicion that an initial angle in the (r, z) plane may be quite important, we repeated the analysis for the particular cases for particles projecting 5° forward from the normal to the field line at the source at Δz = 1 cm, and 5° backward at Δz = 3 cm. The backward-moving ion is essentially useless. For the forward-moving one, however, there is a great increase in available time in the range of source positions for which the ions clear the source radially after precession. Table III is Table II recomputed for this special case. It can be seen that the effect of such an angle is indeed great; if we assume that the above choices of 5° and Δz = 1 cm represent an average for the front end of the source and that there is no contribution from the back end, the effective time is about 700 μsec. This is made possible by the fact that ions can miss the source radially even though the excursions in z remain large. It should be pointed out, however, that the injection period ends at close to half peak field, so that after compression the plasma would be about 10 cm in radius with many particles at only 20 kv energy.

JITTER

A nonadiabatic effect of some interest is the fact that even in a static field the ions do not always reflect at the same values of z and of radial position of the guiding center. The true z_{max} is related to the phase of the ion in its circular path at reflection,[c] and since this phase varies greatly from one transit to the next, the successive values of z_{max} vary in a somewhat chaotic fashion; thus the name "jitter." It can be beneficial in permitting a certain number of borderline cases to survive or harmful in cutting out others that would have been safe otherwise. We have examined the magnitude of the effect for a few

[c]As a rule, z_{max} is greatest when the particle reflects at the point of its circle farthest from the axis. Also all reflections occur fairly near this phase.

Table III

Time intervals available for injection for $\Delta z = 1$ cm and initial direction 5 deg forward[a]

	γ	V_f	V_i	t_f	t_i	Δt (μsec)	$(\Delta t)_{Av}$ (μsec)
z = 10 cm	0	0.070	0.570	2280	280	2000	
	10	0.070	0.295	2280	540	1740	
	20	0.070	0.105	2280	1520	760	
	30	-	-	-	-	-	
	40	-	-	-	-	-	440
z = 15 cm	0	0.082	0.495	1950	320	1630	
	10	0.075	0.495	2140	320	1820	
	20	0.075	0.232	2140	690	1450	
	30	0.075	0.140	2140	1140	1000	
	40	0.075	0.090	2140	1780	360	660
z = 20 cm	0	0.137	0.432	1170	370	800	
	10	0.090	0.432	1780	370	1410	
	20	0.077	0.387	2080	410	1670	
	30	0.077	0.255	2080	630	1450	
	40	0.077	0.202	2080	790	1290	700
z = 25 cm	0	-	-	-	-	-	
	10	0.170	0.367	940	440	500	
	20	0.115	0.367	1400	440	960	
	30	0.095	0.367	1680	440	1240	
	40	0.087	0.367	1840	440	1400	425
z = 30 cm	0	-	-	-	-	-	
	10	-	-	-	-	-	
	20	0.262	0.302	610	530	80	
	30	0.210	0.302	760	530	230	
	40	0.157	0.302	1020	530	490	70

[a] This is taken as representative of the front half of the source; the back half contributes nothing since ions are presumed to be injected backwards there.

cases in the interesting range: for $V = 0.4$, the over-all variation in z is 2 cm at a z of 20 cm, decreasing to 0.6 cm at a z of 6 cm, while at $V = 0.2$ the variation is negligibly small. Since the source will lie on a flux line the jitter should not have much effect on the radial separation of the orbit and the source at successive reflections. For most times of interest the jitter effect is probably small; we have not attempted to explore it further.

CHANGE IN INJECTION ENERGY AND IN RATE OF FIELD RISE

Using a different (but constant) injection energy changes the foregoing arguments in two ways. Increasing the energy to produce the same orbits at later times increases the acceptance times of Table I proportionally. On the other hand, the precession per transit is the same for the same geometrical orbit, but the shrinkage in r and z per transit decreases because the time per transit decreases and simultaneously the magnetic field is greater in magnitude. As a result, the precessional curves in Fig. 1 bounding the useful area on the left will move to the right, further restricting the useful area. We have not attempted any quantitative analysis at a different energy, but a comparison of Tables I and II shows that at 10 kv the precessional curves limit the acceptance times somewhat, though not drastically, over a considerable range in z. We guess, therefore, that the competing effects are rather well balanced at 10 kv, and there is probably not much to be gained in total accepted charge by going higher or lower.

A similar argument applies to the rate of rise of magnetic field. A slower rise would increase the times of Table I proportionally, but the shrinkage per transit decreases and the left-hand bounding curves again move to the right. Therefore we again conclude that, everything else (such as charge exchange) neglected, there is probably not much to gain by changing the rate of rise.

VARIABLE INJECTION ENERGY

It also does not look as though there is much to be gained in total charge injected by programming the injection energy. The reason is seen most strikingly in Table III. Injection begins at about 400 μsec, lasting to 2000 μsec in the most favorable case. If 10 kv or so is the peak voltage to be considered, the best one could hope for would be to utilize the first 400 μsec with an increase in total charge of 400/1600 = 25%. Moreover, if charge exchange is important, the ions of low initial energy are susceptible for the longest time. Finally, according to the adiabatic compression laws, the early ions would actually lower the average energy of the final distribution, though they would be concentrated more densely.

The figures in Table III represent an extreme case, but a look at all the tables shows that where there is an adequate acceptance time at 10 kv, filling earlier times by programming will not increase the total charge by more than a factor of two. However, it has been pointed out by Eby and Damm that it might be possible to improve the chances for nuclear reactions by programming in such a way that the orbits always intersect the axis of the machine.

MULTIPLE SOURCES

It is not clear that one can gain appreciably in total charge by introducing more sources. Referring to Fig. 1, we see that the left-hand bounding curves move to the right as the total allowed precession decreases from 360°. For two sources 180° apart, the $\delta z = 1$ cm boundary moves to the position of the $\delta z = 2$ cm curve, and so on. The $\gamma = 0$ curve for radial shrinkage moves out to 20 cm. This leaves some area available, but not much. Figure 4 shows the resulting curves for this case of two sources. An analysis similar to that described above for one source shows that the effective injection time for each source is approximately cut in half, so that the total charge accepted would be about the same.

One could also introduce a second source at such a position in r and z that it does not interfere with the trajectories from the first source, and vice versa. This procedure seems to us less likely to be harmful, but if the first source is in optimum position, the second will not contribute as much as the first.

β, THERMALIZATION, NUCLEAR REACTIONS

If we adopt the largest of the various computed acceptance times, 700 μsec, and a source current of 1/6 amp, the total number of injected particles is 7×10^{14}. The volume after compression for this case is 1.5×10^4 cm^3, giving a density of 4×10^{10} and an average energy of 35 kv (ranging from 15 to 80 kv). The thermalizing time[6] is 30 sec; the dependence of this time on the various parameters of the system is not great enough to change this time downward by an order of magnitude, so that one can to the first approximation ignore the effect of Coulomb collisions on the ion orbits for 100 msec or so.

In this case β does not mean much, for there is really no temperature to the system. Nevertheless we have $n\overline{W}/(B^2/8\pi) \sim 10^{-4}$, which is still a rough measure of the "loading" of the containing fields.

The number of nuclear reactions is still harder to predict, for $\overline{\sigma v}$ depends strongly on the way in which the various compressed orbits intersect one another. Having nothing better to go by, we adopt $\overline{\sigma v} = 10^{-17}$ cm^3/sec (temperature of 50 kv); this yields the result

$$\frac{dN}{dt} = 2 \times 10^5 \text{ milliseconds.}$$

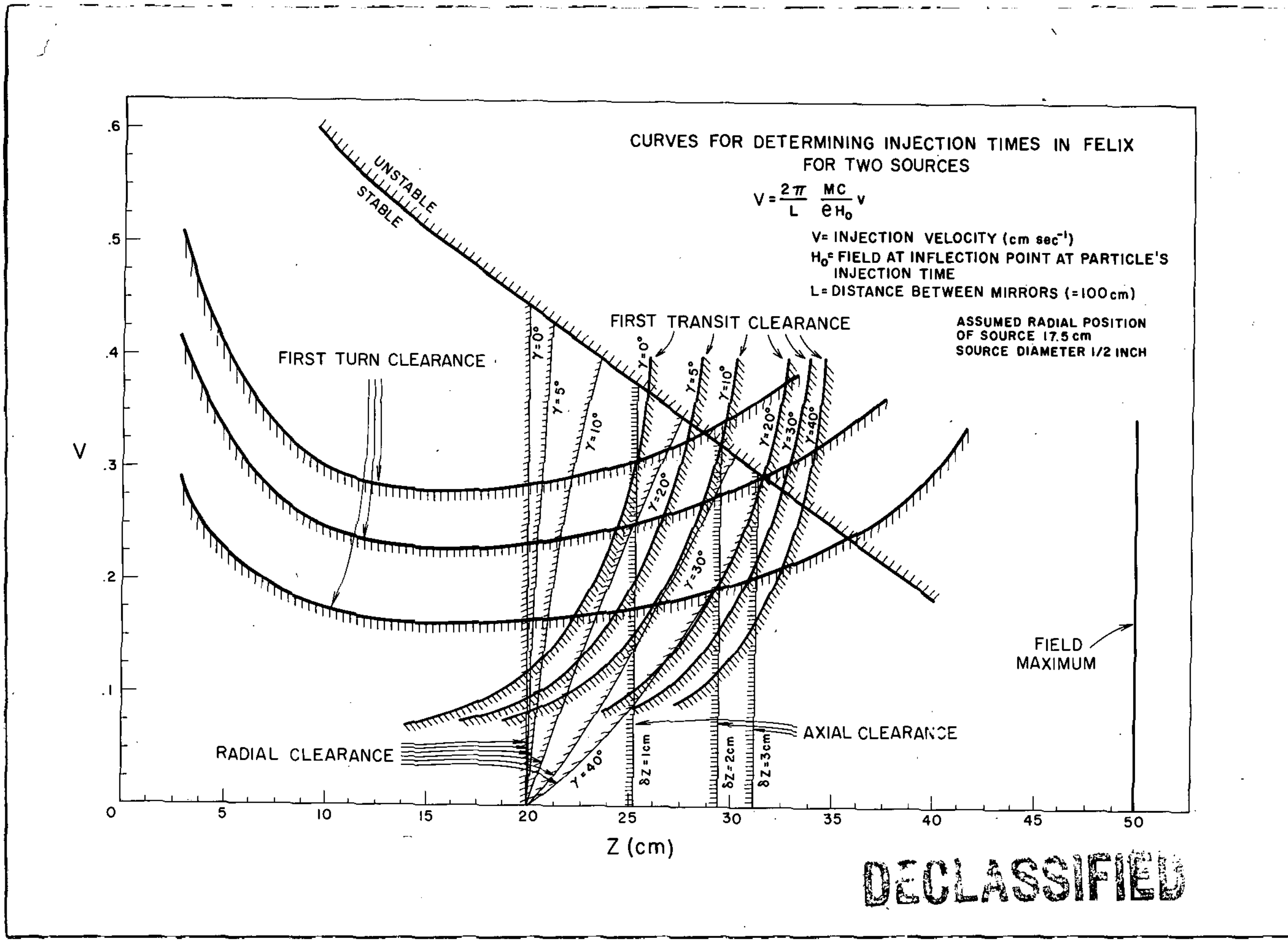
CURVES FOR DETERMINING INJECTION TIMES IN FELIX
FOR TWO SOURCES
$V = \frac{2\pi}{L} \frac{MC}{eH_0} v$
V= INJECTION VELOCITY (cm sec⁻¹)
H_0= FIELD AT INFLECTION POINT AT PARTICLE'S INJECTION TIME
L= DISTANCE BETWEEN MIRRORS (=100 cm)
ASSUMED RADIAL POSITION OF SOURCE 17.5 cm
SOURCE DIAMETER 1/2 INCH
UNSTABLE
STABLE
FIRST TRANSIT CLEARANCE
FIRST TURN CLEARANCE
RADIAL CLEARANCE
AXIAL CLEARANCE
FIELD MAXIMUM
V
Z (cm)
DECLASSIFIED

Fig. 4.

One might as reasonably estimate yield by assuming, for instance, that 10 % of the ions have 80 kv energy and the rest are effectively standing still. On this basis the yield is $\sim 10^4$/millisecond.

The yields are expressed as rates to avoid the question of loss during and after compression due to charge exchange. The presence of neutrals can be quite serious; at a neutral deuterium density of 10^{10} (10^{-7} mm) the lifetime against charge exchange would be of the order of one millisecond.

CONCLUDING REMARKS

It would appear that the rate of rise of field and the injection energy have been well chosen to optimize the total trapped charge. Any substantial improvement would have to come from an increase in injected current, resulting in a linear increase of charge and β, and a quadratic increase in reaction rate.

It should be pointed out that the conclusions of this report are based on the assumption that the charge of the injected ions is neutralized by a corresponding number of electrons. Since the electric fields associated with the charge densities stated in the preceding section would overwhelm the magnetic forces, it is essential that a high degree of neutralization be attained. Since it is not clear that this will come about automatically, there exists the very real possibility that Felix will not perform as well as predicted unless means are found to supply the necessary electrons.

ACKNOWLEDGMENTS

We are indebted to Mrs. Julia Kleinecke and Mr. Robert Weir for their assistance in the numerical computations.

This work was performed under aupsices of the U.S. Atomic Energy Commission.

REFERENCES

1. Reported in part in TID-7536 (Pt. II), p. 170.

2. Post, R. F., Sixteen Lectures on Controlled Thermonuclear Reactions UCRL-4231 (Feb. 2, 1954), Chapter II.

3. Post, R. F. UCRL-4623; UCRL-4723 (to be published)

4. WASH-289, p. 206

5. Alfven, H., Cosmical Electrodynamics, Oxford Univ. Press (1950), p. 21.

6. Spitzer, Lyman, Jr., Physics of Fully Ionized Gases, Interscience Publishers Inc., New York (1956), p. 78.

FIGURE CAPTIONS

Fig. 1. Curves for determining injection times in Felix.

Fig. 2. Precession per transit in Felix.

Fig. 3. Ion-source geometry.

Fig. 4. Curves for determining injection times in Felix for two sources.

DECLASSIFIED

DECLASSIFIED